Malaysian Journal of Analytical Sciences (MJAS)
Published by Malaysian Analytical Sciences Society

THE EFFECT OF ANTHRACENE GROUP SUBSTITUTION OF DISUBSTITUTED CHALCONE DERIVATIVE FEATURING TEREPHTHALALDEHYDE π-LINKER ON NON-LINEAR OPTICAL (NLO) CHARACTERISTIC

(Kesan Penggantian Kumpulan Antrasena Atas Terbitan Kalkon Dualgantian Yang Menampilkan Terephthalaldehid π-Penyambung Keatas Ciri-Ciri Optik Bukan Linear)

Nurul Nabilah Shuaib[1], Adibah Izzati Daud[1*], Suhana Arshad[2], Mohamad Aizat Abu Bakar[3], Wan M. Khairul[4]

[1]Faculty of Engineering and Chemical Technology,
Universiti Malaysia Perlis,
02600 Arau, Perlis, Malaysia.
[2]School of Physics,
Universiti Sains Malaysia, 11800 USM, Pulau Pinang, Malaysia.
[3]Institute of Nano Optoelectronics Research and Technology (INOR),
Universiti Sains Malaysia, 11800 USM, Penang, Malaysia
[4]Faculty of Science and Marine Environment,
Universiti Malaysia Terengganu, 21030 Kuala Nerus, Terengganu, Malaysia.

[*]Corresponding author: adizzati@unimap.edu.my

Received: 22 September 2022; Accepted: 17 January 2023; Published: 22 February 2023

Abstract

In past years, the π-conjugated system has attracted much attention as a promising material for developing and manufacturing the next generation of organic electronics made of synthesised organic compounds. Chalcone, having the π-conjugated systems in their molecular structures and the unique α, β-unsaturated ketone structural, have gained much attraction due to their potential use in optoelectronics applications like organic light emitting diode (OLED). By altering the molecular structure, the physical and chemical properties of chalcone derivatives can be tailored to the application needed. In recent years, chemists have produced many types of π-conjugated molecules to acquire excellent luminescence characteristics from organic compounds, and such structures typically lead to intense colour and excellent photoluminescence. In this study, a disubstituted chalcone derivative featuring terephthalaldehyde (**N1A**) as a π-linker with anthracene as donating group substitution has been synthesised through the Claisen-Schmidt condensation reaction. The synthesised compound has been characterised using Fourier Transform Infrared spectroscopy (FTIR) and UV-Visible analysis. Density functional theory (DFT) computations are executed to evaluate the effect of anthracene as an electron donating substitution on NLO properties of disubstituted chalcone derivative. NLO responses of this disubstituted chalcone derivative disclose that the chalcone molecular framework exhibit an important characteristic for further application as OLED emitting material.

Keywords: chalcone, density functional theory, non-linear optical, spectroscopic

Abstrak

Pada tahun-tahun lepas, sistem π-konjugasi telah menarik banyak perhatian sebagai bahan yang berpotensi untuk dibangunkan dan dikeluarkan sebagai generasi seterusnya elektronik organik, yang dibuat daripada sintesis sebatian organik. Kalkon, yang mempunyai sistem terkonjugasi-π dalam struktur molekulnya serta struktur keton α, β-tak tepu yang unik, telah mendapat banyak tarikan kerana potensi penggunaannya dalam aplikasi optoelektronik seperti diod pemancar cahaya organik (OLED). Dengan mengubah struktur molekul, sifat fizikal dan kimia, terbitan kalkon boleh disesuaikan dengan aplikasi yang diperlukan. Dalam tahun-tahun kebelakangan ini, ahli kimia telah menghasilkan banyak jenis molekul terkonjugasi-π untuk memperoleh ciri kependarkilauan yang sangat baik daripada sebatian organik, dan struktur sedemikian biasanya membawa kepada warna yang terang dan foto pendarcahaya yang sangat baik. Dalam kajian ini, terbitan kalkon tergantian yang menampilkan terephthalaldehid (**N1A**) sebagai penghubung-π dengan antrasena sebagai penggantian kumpulan penderma, telah disintesis melalui tindak balas pemeluwapan Claisen-Schmidt. Sebatian yang disintesis telah dicirikan menggunakan spektroskopi Lembayung Inframerah (FTIR) dan analisa Ultra Lembayung sinar nampak. Pengiraan teori fungsi ketumpatan (DFT) dilaksanakan untuk menilai kesan antrasena sebagai penggantian pendermaan elektron ke atas sifat NLO bagi terbitan kalkon tersubstitusi. Dapatan NLO bagi terbitan dualgantian ini menunjukkan kerangka molekul kalkon mempunyai ciri penting untuk aplikasi seterusnya sebagai bahan pemancar OLED.

Kata kunci: kalkon, teori fungsi ketumpatan, optik bukan linear, spektroskopi

Introduction

Light emitting diode (LED) represents a little solid-state semiconductor device that produces light when current flows through it [1]. The current produced is due to the movement of electrons through a semiconductor. An inorganic semiconductor is commonly used in LED. Haque et al. reported that using inorganic semiconductors in LED has several problems in terms of efficiency, heat management, colour rendering, lifetime, and probably the most significant one is the high cost [2]. In contrast, LED that uses an organic semiconductor is called organic light emitting diode (OLED), which was first revealed by Pope, Kallmann, and Magnante in 1963 [2]. Organic semiconductors are polymers or π-bonded molecules and can conduct electricity when charge carriers are injected into them [3]. Organic semiconductor devices now form the basis of an ongoing revolution in electronics in the twenty-first century. One of the materials used in organic electronics is organic materials that are made up of carbon-based materials. The widely used inorganic materials in semiconductors have caused some disadvantages as it needs high purity and accurate processing under extremely demanding conditions. The problems arising when using inorganic semiconductors have led to extensive semiconductor technology development. Hence, the organic semiconductors are wished for the potential solutions, especially on how the organic compound in these organic semiconductors will affect the OLED performance. Some benefits of using organic semiconductors are infinite variety and tuneable properties by changing the chemical structure, easy shaping, and manufacturing. These benefits came from the great properties of organic materials [4].

Organic materials such as chalcone having π-conjugated materials have become a major interest in OLED applications due to their low cost, tuning ability, structural diversity, favourable chemical modification, flexibility, and ease of fabrication. Chalcone derivatives occur naturally in plants and can also be synthesised using a synthetic approach to produce fluorescent materials. The characteristics of chalcone, particularly having benefits of chemical structure modification, have raised a question on how the modified structure can change the effect chalcone derivatives have on that particularly applied field. Organic materials having well-defined electrical properties are being deployed for optoelectronic devices such as OLED, and these devices are now replacing the use of liquid crystal displays (LCD) in consumer electronics such as cell phones, tablets, and televisions [5]. In past years, the π-conjugated system has attracted much attention as a promising material for developing and manufacturing the next generation of electronics, such as organic electronics. Organic semiconductors possess structural plasticity that allows the molecular design to incorporate functionality [6]. Aside from that, π-conjugated systems in molecular structures have received much attention due to their use in optoelectronics like OLEDs. The

conjugated organic molecules are used in organic electronics. Furthermore, by altering the molecular structure, the physical and chemical properties of organic molecules can be customised to the application's needs. For example, the colour of organic molecules' emission can be changed by increasing or lowering the π-electron conjugation [7]. Over the last 150 years, chemists have produced many types of π-conjugated molecules to acquire excellent luminescence characteristics from organic compounds, and such structures typically lead to intense colour and excellent photoluminescence [8]. In addition, Cho et al. stated that it has recently been discovered that even minor chemical changes can significantly impact luminescence characteristics [9].

It is worth noting that chalcones have a unique structure with an α, β - unsaturated carbonyl framework that helps with structural alterations [10]. By modifying the polarity of aprotic solvents, heteroaryl chalcones containing both electron donor and acceptor groups have been studied, which improves quantum yields and fluorescence intensity via intermolecular charge transfer (ICT) [11]. As a result, the researchers are working on chalcone structural alteration in developing new and unique materials with a wide range of uses. This structural modification also includes the electron donating-withdrawing substituents that will affect the luminescent properties of chalcone derivatives. According to Prabhu et al., it is clear that the electron-donating group significantly influences the optical properties of the chalcones [12]. Therefore, a comprehensive understanding of the relationship between conjugated π-linker and molecular design is a crucial concern for developing efficient luminescent materials in chalcone derivatives for high OLED performance.

In this study, a new disubstituted chalcone derivative; ((2E,2'E)-3,3'-(1,4-phenylene) bis(1-(anthracen-9-yl) prop-2-en-1-one) (**N1A**) has been successfully synthesised. This study aims to characterise and elucidate the disubstituted chalcone derivative using Fourier Transform Infrared spectroscopy (FTIR) and Ultraviolet-Visible (UV-vis) spectroscopy. The nonlinear optical (NLO) properties such as nonlinear refractive (μ), nonlinear absorption (β) and third-order nonlinear susceptibility (χ^3) of the disubstituted chalcone derivative are evaluated through the Z-scan method. Moreover, the density functional theory (DFT) method is computed using B3LYP/6-31G (d, p) basic set to obtain the optimised geometric molecular structure before analysing the NLO response.

Materials and Methods

Chemical and reagents

All starting chemicals, reagents, and solvents were purchased and used as received from Sigma-Aldrich and Merck which are 9-acetylphenanthrene, terephthalaldehyde, ethanol, sodium hydroxide, acetonitrile, and dichloromethane. All of the chemicals, reagents, and solvents were used as received without further purification.

Experimental details

Disubstituted chalcone is prepared using the Claisen-Schmidt condensation reaction method because it is affordable, simple to use, and not sensitive to oxygen or water, making it simple to operate at room temperature and readily applicable in laboratories [13]. 9-Acetylanthracene (7.5 mmol, 1.6 g) and terepthalaldehyde (3.7 mmol, 0.5 g) were each dissolved in ethanol (10 mL). Both mixtures are mixed before adding ethanol (50-60 mL) until the mixture is completely dissolved. While stirring, a catalytic amount of 20% NaOH was added to the solution dropwise. The reaction mixture was stirred for 5 hours at room temperature. Once adjudged completed, the reaction mixture was poured into cold iced water and left for precipitation. The resultant crude product was filtered. The obtained crude product of **N1A** was recrystallised from acetonitrile by a slow evaporation process to afford the corresponding disubstituted chalcone derivative (**N1A**). Scheme 1 illustrates the synthetic pathway to the synthesis of **N1A**.

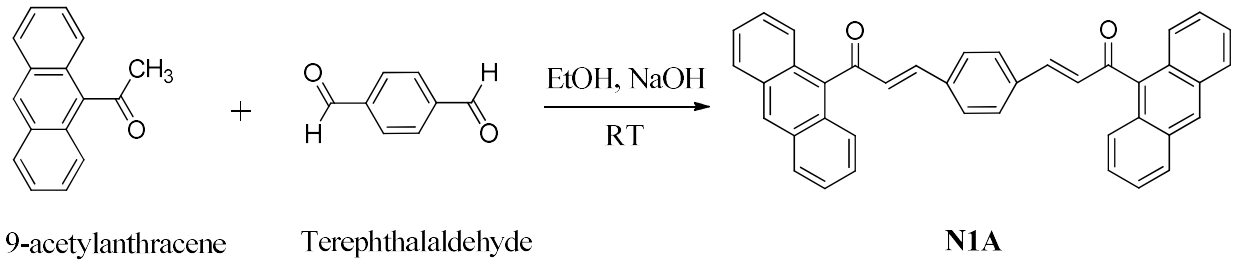

9-acetylanthracene Terephthalaldehyde **N1A**

Scheme 1. Synthesis of disubstituted chalcone derivative (**N1A**)

Instrumentation and characterisation

The chemical structure of the **N1A** chalcone is confirmed by recording its FTIR spectra. KBr pellet is used on Perkin Elmer Spectrum Version 10.03.06 to obtain FTIR spectra in the wavenumber range at 4000-650 cm^{-1}, and the infrared values are listed in $\bar{\upsilon}$ units. The UV–Vis absorption spectrum was observed in acetonitrile (CH_3CN) solutions at room temperature respectively on Perkin Elmer Lambda 365 UV–Vis Spectrophotometer in the range of 200-700 nm at a concentration of 10^{-5} mol L^{-1} in 1 cm cuvette.

The third-order NLO properties of **N1A** chalcone are evaluated using the Z-scan technique. The transmittance of a nonlinear medium is measured with this method as a function of the sample position using a single polarised Gaussian laser beam in a tight focus geometry. This single beam, which is propagating in the Z direction, is narrowly concentrated. The sample is moved in the Z direction, and a finite aperture in the far field is used to measure the transmitted intensity as a function of the sample's Z position, measured with reference to the focal plane. Self-focusing or self-defocusing changes the wavefront phase when the sample passes through the beam focus (at Z = 0), changing the observed beam intensity [13]. A continuous wave from a diode-pumped solid-state laser operating at 532 nm is used to analyse the NLO response in the **N1A** chalcone. The sample was kept in a quartz cuvette with a path length of 1 mm, and the beam was sharply focussed with a 20 cm focusing lens. A laser beam profiler measured the beam waist at the focal point [14]. A powdered sample weighing 0.002 g was used for the analysis in 1 mL acetone. The experiments were conducted at room temperature. The sample used in this experiment is $4x10^{-3}$ M of acetone solution of **N1A**. The Z-scan technique measures nonlinear absorption (NLA) and nonlinear reflection (NLR). This technique was used to explore third-order susceptibility (χ^3), nonlinear refractive index (n_2), and nonlinear absorption coefficient (β).

The basic single-beam Z-scan setup is shown in Figure 1 [15]. The normalised transmittance was plotted by Levenberg–Marquardt algorithm to estimate the effective nonlinear absorption β_{eff} value. From the value of nonlinear absorption (β) and nonlinear refractive (n_2), the imaginary and real part of third-order nonlinear susceptibility, $\chi^{(3)}$, can be obtained from the following equation (Eq. 1 – Eq. 3):

$$Re\,\chi^{(3)}\,(\text{esu}) = [10^{-4}(\varepsilon_0 C^2 n_0^2 n_2]/\pi \quad \text{(Eq. 1)}$$

$$Im\,\chi^{(3)}\,(\text{esu}) = [10^{-2}(\varepsilon_0 C^2 \beta\lambda]/\pi \quad \text{(Eq. 2)}$$

$$\chi^{(3)} = [(Re\,\chi^{(3)})^2 + (Im\,\chi^{(3)})^2]^{1/2} \quad \text{(Eq. 3)}$$

where C is the velocity of the light in a vacuum, ε_0 is the permittivity of the free space, and n_0 is the linear refractive index of the sample solution.

The optimisation of the molecular geometries leading to energy minima was achieved using the DFT method with a basic set of B3LYP/6-31G (d, p) level of theory as implemented in the GAUSSIAN 09 program

package. The optimised structural parameters were used to calculate the vibrational wavenumbers [16]. The nonlinear optical properties such as static dipole moments (μ_{tot}), mean polarizability ($<\alpha_{tot}>$), anisotropic polarizability ($\Delta\alpha$) and first hyperpolarizability index (β-V), were computed via B3LYP/6-31G (d, p) level of theory under finite field scheme at $\omega = 0$, and the values obtained were calculated using the following equations (Eq. 4 – Eq. 7):.

$$\mu_{tot} = \left(\mu_x^2 + \mu_y^2 + \mu_z^2\right)^{1/2} \quad \text{(Eq. 4)}$$

$$< \alpha_{tot} > = \frac{1}{3}\left(\alpha_{xx} + \alpha_{yy} + \alpha_{zz}\right) \quad \text{(Eq. 5)}$$

$$\Delta\alpha = \frac{1}{\sqrt{2}}\left[\left(\alpha_{xx} - \alpha_{yy}\right)^2 + \left(\alpha_{yy} - \alpha_{zz}\right)^2 + \left(\alpha_{zz} - \alpha_{xx}\right)^2 + 6\left(\alpha_{xy}^2 + \alpha_{xz}^2 + \alpha_{yz}^2\right)\right] \quad \text{(Eq. 6)}$$

$$\beta - V = \left(\beta_x^2 + \beta_y^2 + \beta_z^2\right)^{1/2} \quad \text{(Eq. 7)}$$

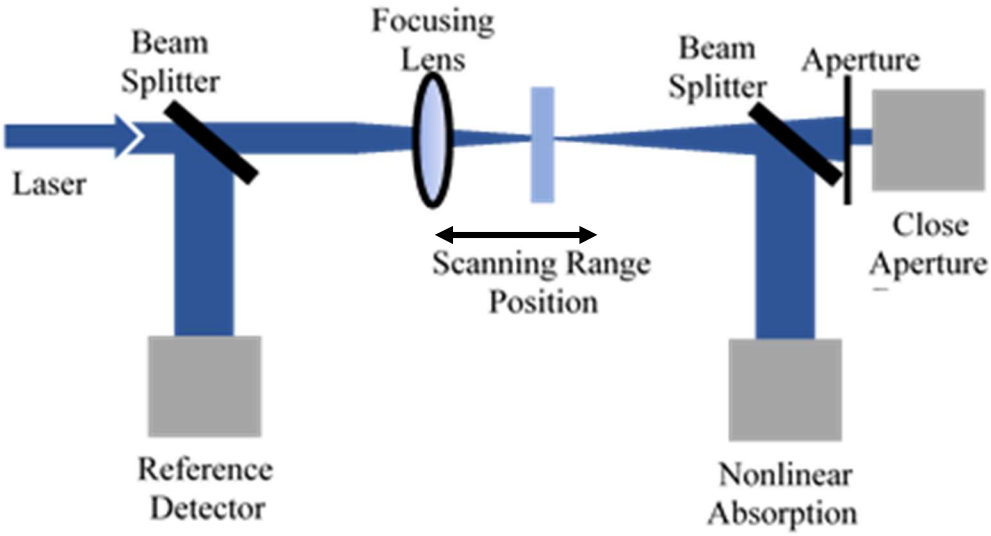

Figure 1. The setup for Z-scan analysis

Result and Discussion

Vibrational analysis

The FTIR spectrum of **N1A** is shown in Figure 2. The stretching frequency of α, β-unsaturated carbonyl compounds usually lie in the range of 1660-1685 cm^{-1}. The stretching frequency of **N1A** gives away characteristics -C=O stretching at 1645 cm^{-1} and -C=C- stretching at 1586 cm^{-1}. The carbonyl group mostly depends on the bond strength, which depends on steric effects, inductive effects, conjugative effects, and oxygen lone pair electrons. This might be the reason for the difference in wavelength in the **N1A** chalcone. However, the wavelength still agrees with the literature value of 1600 cm^{-1}. The C=C stretching vibration is probably around 1667-1640 cm^{-1}. However, C=C is expected around 1600 cm^{-1} when conjugated with C=O. Additional -C=C- stretching and the aromatic C-H in-plane and out-of-plane bending bands of aromatics C-H at 1108 cm^{-1} and 734 cm^{-1}, respectively [17], had established due to the frequent occurrence of aromatic rings in all compounds, especially in **N1A** chalcones. The typical ranges for the C-H in-plane and out-of-plane bending vibrations are 1300-1000 cm^{-1} and 1000-700 cm^{-1}, respectively. The type of substituents has no impact on the bands in this region. Due to the inductive effect that increases the substituent's chain length, all C-H stretching is weak [18]. The vibrational modes for the **N1A** chalcone are presented in Table 1.

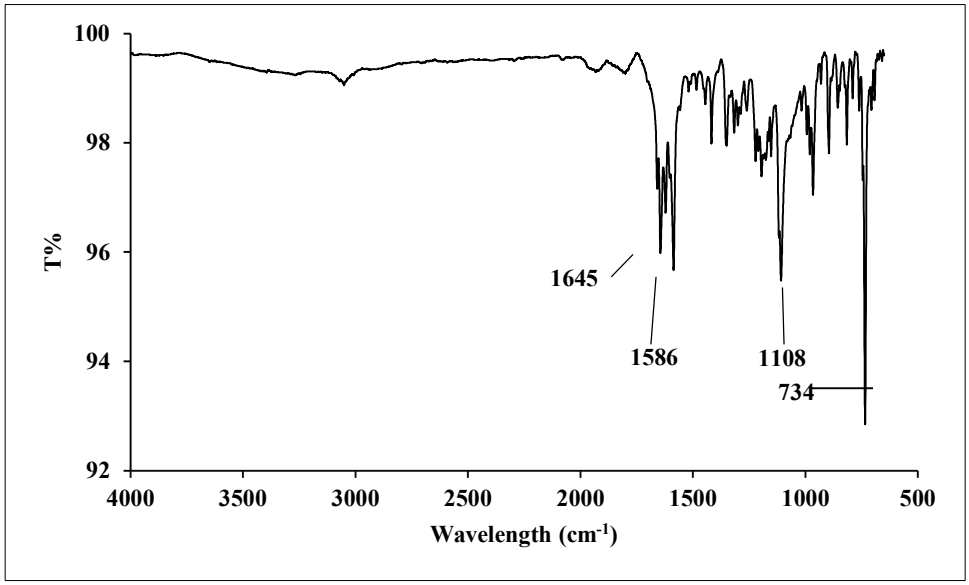

Figure 2. The FTIR spectrum of **N1A**

Table 1. Vibrational Mode for **N1A** chalcone.

Vibrational Mode	N1A
	Wavelength (cm^{-1})
C=O stretch	1645
C=C-C aromatic ring stretch	1586
C-H in-plane band	1108
C-H out-of-plane band	734

Electronic transition analysis

The UV-vis absorption spectrum of **N1A** is shown in Figure 3. It is clear that **N1A** chalones are transparent in the entire visible region and the absorption takes place in the UV region. The absence of absorption in the visible region is a key factor if any compound is to be exploited for NLO applications at room temperature [19]. Most organic compound absorption spectroscopy is based on transitions of n or π-electrons to the π* excited state. As a result, the transition absorption peaks occur within 200–700 nm suitable for experimental investigation. In order to supply the electrons for these transitions, the molecule must have an unsaturated group. α, β-unsaturated carbonyl compounds usually show two absorption bands of the n→π* and π→π* transitions [20]. The absorption and transmission spectra help us to identify the nature of the molecule by analysing the transition of electrons in σ and π orbitals between the ground state and higher excited states with the energy absorbed [21]. The UV-Vis absorption spectra of **N1A** exhibit one absorbance maximum, as shown in Figure 3, at 252 nm. The maximum absorption of **N1A** chalcone at 252 nm is due to the increased conjugation and greater resonance stabilisation. This peak might attribute to π→π* transition since the wavelength is below 300 nm, indicating the presence of a carbonyl group in the compound. The other absorbance bands observed are 341 nm, 367 nm and 384 nm. The absorbance bands observed have an absorption tail stretching to ± 454 nm. The peaks may be attributed to the mixture transition of n→π* and π→π* interband transition and are due to the excitation in the aromatic

rings for wavelengths more than 300 nm. N1A chalcone exhibits a higher maximum wavelength due to its greater amount of benzene rings. The absorption corresponds to the transition from the highest occupied molecular orbital (HOMO) in the ground state to the lowest unoccupied molecular orbital (LUMO) in the excited state [21]. As the molecule is conjugated, the HOMO-LUMO transition implies the transfer of electron charge density throughout the aromatic rings [22].

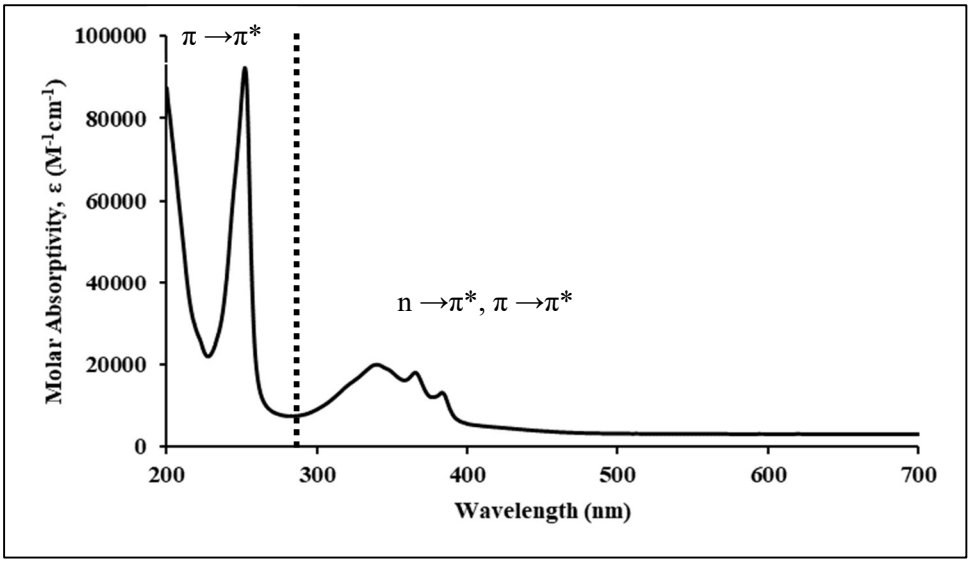

Figure 3. UV-Vis spectrum and electronic transition of **N1A** chalcone

Table 2. electronic transition of **N1A** chalcones

Compound	λ (nm), ε (M^{-1} cm^{-1})	Electronic transition
N1A	252, 92134	π→π*
	341, 19810	n→π*, π→π*
	367, 17381	n→π*, π→π*
	384, 12889	n→π*, π→π*

Optical energy band gap (E_g) analysis

The strongest absorption and smaller energy gap, particularly in the visible region, are important features in the suitability for optoelectronic applications [23]. The purpose of evaluating the energy band gap (E_g) is to calculate the difference in orbital energy between the highest occupied molecular orbital (HOMO) (the top of the valence band) and its lowest unoccupied molecular orbital (LUMO) (the bottom of the conduction band). Since they have a greater capability for electron mobility in the π-conjugated system, compounds with shorter HOMO-LUMO energy gaps are highly preferred because they produce an enlarged energy distribution [24]. The optical band gap was calculated via Tauc's approach (Figure 4) by analysing the UV-vis spectra to determine the absorption coefficient (α) and photon energy ($h\nu$). This technique entails extrapolating the linear stretch of the tail of the lower energy band $(\alpha h\nu)^2$ up to the cut-off value with the abscissa axis, which corresponds to the photon (hν) energy. The absorption coefficient (α) is calculated from the absorbance data, and frequency (ν) is the reciprocal of wavelength, with h being Planck's constant [25]. The optical bandgap for the **N1A** chalcone is 3.16 eV. The optical bandgap plays

an essential role in the enhancement of the NLO properties of the compound. The narrowed bandgap is due to the intermolecular charge transfer (ICT) transition, leading to the high performance of NLO response [26]. Anthracene as donating group substituent, has a greater π-conjugation system, leading to lower optical bandgap energy in the **N1A** chalcone. The optical bandgap was evaluated using the following equation (Eq. 8 – Eq. 10):

$$(\alpha h\nu)^2 = A(h\nu - E_g) \quad \text{(Eq. 8)}$$

$$h\nu = \frac{1240}{\lambda} \quad \text{(Eq. 9)}$$

$$\alpha = 2.303\frac{A}{L} \quad \text{(Eq. 10)}$$

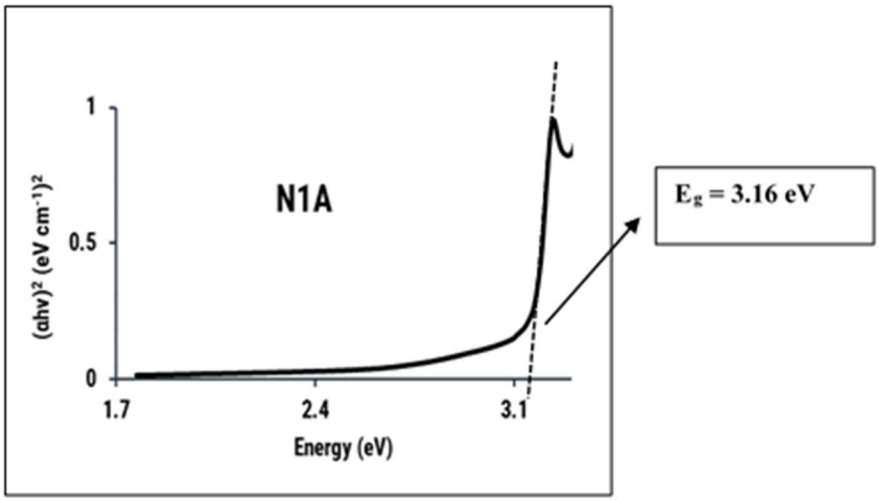

Figure 4. The Tauc's plot for optical energy band gap analysis of **N1A**

Non-linear optical characterisation

The NLO properties were investigated using the Z-scan technique. From Figure 3, the absorption is absent in the region between 500-700 nm which is a key requirement for materials having NLO properties. The linear absorption coefficient, α, of the compound for the 4 x 10^{-3} M was measured to be 0.4604/cm. Figure 5 shows the open (left) and closed aperture (right) transmittance spectra for the **N1A** chalcone. **N1A** chalcone shows a symmetric valley in the open aperture Z-scan spectrum about the focus, indicating positive non-linear absorption in the compound. Maximum absorption typically occurs when the sample is at the focal point of the lens since the on-axial peak irradiance I_0 of the beam is the maximum. The reduction in the transmittance measured with an open aperture is independent of non-linear refraction (NLR) and thus can be used to determine the value of the two-photon absorption (TPA) coefficient (β) by the depth of the valley. By fitting experimental normalised transmission data to the equation described in the literature [27], the value of nonlinear absorption (β) was found to be 2.5 x 10^{-4} cm W^{-1} for **N1A** chalcone. The strong reverse saturable absorption (RSA), which is responsible for the NLO material properties [28], is visible in the sample transmittance profile shown in Figure 5 (right), where the excited state absorption is greater than that for the ground state. This might be due to the effect of the delocalisation of π-electrons in the anthracene group and strong ICT in the compound.

Nonlinear refraction coefficient (n_2) is obtained from the transmittance measurements during close aperture by placing an aperture in front of the detector (closed aperture). The division method is applied to obtain pure nonlinear refraction. The Z-scan spectrum in close aperture is shown in Figure 5. The finding shows a negative nonlinear refraction property in the **N1A** chalcone (defocusing). However, the calculation shows a positive value of nonlinear refraction. The experimental data were fitted with the equation described in the literature, which yields nonlinear refraction, 1.2 x10^{-15} esu. From the value of the imaginary part (Im χ^3) and real part (Re χ^3), the third-order nonlinear susceptibility, $|\chi^3|$, was evaluated to be 2.8 x 10^{-6} esu, which indicates that the material possesses good NLO properties. However, the value is lower due to the donor-pi-donor system compared to the previously reported chalcone derivatives of the D-p-A system [15, 16]. The calculated NLO parameters extracted from Z-Scan curves are shown in Table 3.

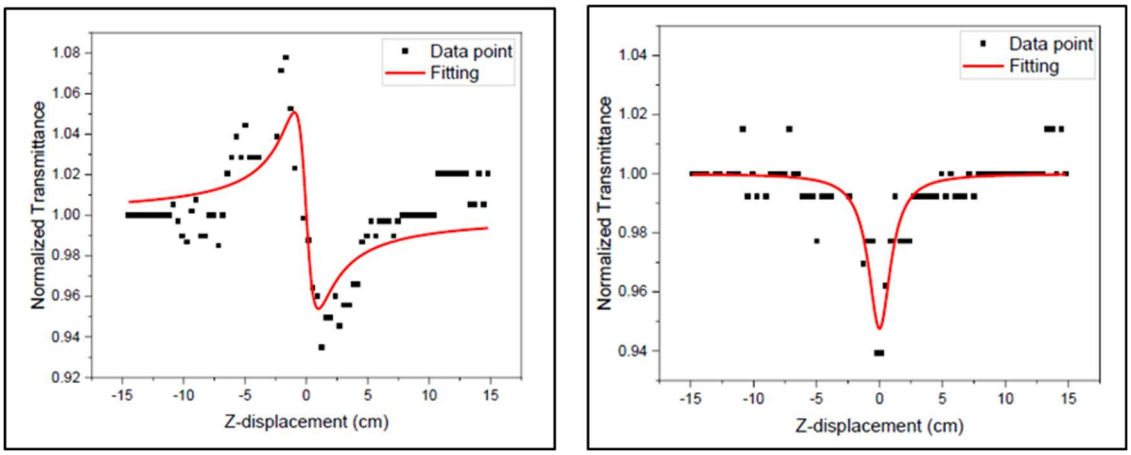

Figure 5. Close (left) and open (right) aperture of Z-scan analysis

Table 3. The calculated NLO parameters extracted from Z-Scan curves

Parameter	Value
Nonlinear absorption [β]	2.5 x10^{-4} cm/W
Nonlinear refraction [n_2]	1.2 x10^{-15} cm^2/W
Imaginary part of third susceptibility [Im $\chi^{(3)}$]	2.8 x10^{-6} esu
Real part of third susceptibility [Re $\chi^{(3)}$]	8.5 x10^{-15} esu
Third-order nonlinear susceptibility [$\chi^{(3)}$]	2.8 x10^{-6} esu

Quantum chemical calculation using density functional theory (DFT)

The nonlinear optical response of a material is strongly correlated with its electric properties, such as its dipole moments, polarizability, and hyperpolarizabilities [29]. When an external field is applied, molecules experience an induced electric dipole moment. This dipole moment is then approximated as the origin to examine microscopic polarizabilities. Additionally, the dipole moment directly affects the hyperpolarizability [30]. In this study, the static dipole moment and polarizability, anisotropic polarizability and hyperpolarizability were computed for the **N1A** chalcone under B3LYP / 6-31G (d, p) method, and the values obtained are presented in Table 4. A higher dipole moment will induce greater polarisation in the field direction. The total dipole moment (μ), mean polarizability (<α>), anisotropy of polarizability (Δα) and hyperpolarizability (β) are found to be 4.49 D, 3.45 x 10^{-23} esu, 3.96 x 10^{-24} esu and 3.53 x 10^{-30} esu, respectively for **N1A** chalcone. The value of

the dipole moment of **N1A** chalcone is higher than the chalcone derivative with anthracene studied by [31] which is 3.18 D. NLO properties can be related to the HOMO-LUMO energy gap and the dipole moment of the molecules. When E_g decreases, NLO properties increase. Smaller E_g allows a higher charge transfer within the electron delocalisation system. Based on Table 4, **N1A** chalcone shows good NLO properties and has the potential in related NLO devices application. DFT study provides a valuable tool for the in-depth examination of new disubstituted chalcone derivative compounds and the electronic property prediction for possible applications.

Table 4. Calculated static dipole moment, polarizability, anisotropic polarizability and hyperpolarizability from DFT data

Compound	Electric dipole moment, μ (debye)	Polarizability, <α> (e.s.u) (x10^{-23})	Anisotropic polarizability, Δα (e.s.u) (x10^{-24})	Hyperpolarizability, β (e.s.u) (x10^{-30})
N1A	4.49	3.45	3.96	3.53

Conclusion

A new chalcone derivative ((2E,2'E)-3,3'-(1,4-phenylene) bis(1-(anthracen-9-yl) prop-2-en-1-one) (**N1A**) was successfully synthesised and characterised for its NLO properties. The functional groups of the C=O carbonyl group, C=C-C aromatic ring, and aromatic C-H of the FTIR spectrum confirmed the structure of chalcone in **N1A** chalcone. The UV-visible study shows that the material is transparent in the visible region with the energy band gap of 3.16 eV and the electron transition analysis revealed the n→π* and π→π* transition of the carbonyl group and the presence of aromatic rings. The NLO response has been explored using a single-beam Z-scan and DFT method. The value of nonlinear absorption (β) and nonlinear susceptibility (χ3) are 2.5 x10^{-4} cmW^{-1} and 2.8 x10^{-6} esu, respectively, while for dipole moment (μ), polarizability (α) and hyperpolarizability (β), the values are found to be 4.49 D, 3.45 x10^{-23} esu and 3.5 x10^{-30} esu, respectively. **N1A** chalcone represents a promising NLO material due to the good NLO response. This NLO characteristic and strong band gap stability of this material are very intriguing for potential use in nonlinear optical devices. In a nutshell, molecular arrangement, the role of donor substituent, and the narrow energy gap may all contribute to the NLO performances.

Acknowledgement

The authors would like to acknowledge the financial support from the Ministry of Higher Education, Malaysia, for the Fundamental Research Grant Scheme (FRGS) FRGS/1/2020/STG05/UNIMAP/02/6, School of Physics and Institute of Nano Optoelectronics Research and Technology (INOR), Universiti Sains Malaysia for assisted in Z-scan analysis, and Universiti Malaysia Perlis for research facilities and support.

References

1. Bagher, A. M. (2017). Quantum dot display technology and comparison with OLED display technology. *International Journal of Advanced Research in Physical Science*, *4*(1): 48-53.
2. Haque, S., Shah, M. S., Rahman, M. and Mohiuddin, M. (2017). Biopolymer composites in light emitting diodes. *Biopolymer Composites in Electronics*, 277-310.
3. Nagar, R., Varrla, E. and Vinayan, B. P. (2018). Photocatalysts for hydrogen generation and organic contaminants degradation. *Multifunctional Photocatalytic Materials for Energy*: pp. 215-236.
4. Chen, F. C. (2018). Organic semiconductors. *Encyclopedia of Modern Optics*: pp. 220-231.
5. Dykstra, E., Fralaide, M., Zhang, Y., Biswas, R., Slafer, W. D., Shinar, J. and Shinar, R. (2022). OLEDs on planarized light outcoupling-enhancing structures in plastic. *Organic Electronics*, 111: 106648.
6. Wang, C., Dong, H., Hu, W., Liu, Y. and Zhu, D. (2012). Semiconducting π-conjugated systems in field-effect transistors: a material odyssey of organic electronics. *Chemical reviews*, 112(4): 2208-2267.

7. Ansari, S. P. and Ali, F. (2018). Conjugated organic polymers for optoelectronic devices. Functional Polymers, edited by MA Jafar Mazumder, H. Sheardown, and A. Al-Ahmed (Springer International Publishing): pp. 1-40.
8. Ahmad, A., Sinha, R. K., Kulkarni, S. D., Lewis, P. M., Bhat, P. and Shetty, N. S. (2022). Synthesis, photophysical properties and DFT studies of chalcones and their 2-methoxy-3-cyanopyridine derivatives. *Journal of Photochemistry and Photobiology A: Chemistry*, 114494.
9. Cho, E., Coropceanu, V. and Brédas, J. L. (2021). Impact of chemical modifications on the luminescence properties of organic neutral radical emitters. *Journal of Materials Chemistry C*, *9*(33): 10794-10801.
10. Rammohan, A., Reddy, J. S., Sravya, G., Rao, C. N. and Zyryanov, G. V. (2020). Chalcone synthesis, properties and medicinal applications: a review. *Environmental Chemistry Letters*, 18(2): 433-458.
11. Pannipara, M., Asiri, A. M., Alamry, K. A., Arshad, M. N. and El-Daly, S. A. (2015). Synthesis, spectral behaviour and photophysics of donor–acceptor kind of chalcones: excited state intramolecular charge transfer and fluorescence quenching studies. *Spectrochimica Acta Part A: Molecular and Biomolecular Spectroscopy,* 136: 1893-1902.
12. Prabhu, A. N., Upadhyaya, V., Jayarama, A. and Bhat, K. S. (2016). Third-order NLO property of thienyl chalcone derivative: Physicochemical analysis and crystal structure determination. *Molecular Crystals and Liquid Crystals,* 637(1), 76-86.
13. Al-Ahmad, A. Y., Shabeeb, G. M., Abdullah, A. Q. and Ziadan, K. M. (2011). Z-scan measurement for the nonlinear absorption and the nonlinear refraction of poly1, 4-diazophenylene-bridged-tris (8-hydroxy-quinoline) aluminum (PDPAlq3). *Optik*, 122(21): 1885-1889.
14. De Araújo, C. B., Gomes, A. S. and Boudebs, G. (2016). Techniques for nonlinear optical characterization of materials: a review. *Reports on Progress in Physics*, 79(3): 036401.
15. Alsaee, S. K., Bakar, M. A. A., Zainuri, D. A., Anizaim, A. H., Zaini, M. F., Rosli, M. M. and Razak, I. A. (2022). Nonlinear optical properties of pyrene-based chalcone:(E)-1-(4′-bromo-[1, 1′-biphenyl]-4-yl)-3-(pyren-1-yl) prop-2-en-1-one, a structure-activity study. *Optical Materials*, 128: 112314.
16. Anizaim, A. H., Arshad, S., Zaini, M. F., Abdullah, M., Zainuri, D. A. and Razak, I. A. (2019). Third order nonlinear optical properties of selected fluorinated chalcone derivatives. *Optical Materials*, 98: 109406.
17. Kumar, P. R., Ravindrachary, V., Janardhana, K. and Poojary, B. (2012). Structural and optical properties of a new chalcone single crystal. *Journal of Crystal Growth*, 354(1): 182-187.
18. Sabina, X. J., Karthikeyan, J., Velmurugan, G., Tamizh, M. M. and Shetty, A. N. (2017). Design and in vitro biological evaluation of substituted chalcones synthesized from nitrogen mustards as potent microtubule targeted anticancer agents. *New Journal of Chemistry*, 41(10): 4096-4109.
19. Chinnasami, S., Manikandan, M., Chandran, S., Paulraj, R. and Ramasamy, P. (2019). Growth, Hirshfeld surfaces, spectral, quantum chemical calculations, photoconductivity and chemical etching analyses of nonlinear optical p-toluidine p-toluenesulfonate single crystal. *Spectrochimica Acta Part A: Molecular and Biomolecular Spectroscopy*, 206: 340-349.
20. Sawant, A. B. and Nirwan, R. S. (2012). Synthesis, characterization and DFT studies of 6, 8-dichloro-2-(4-chlorophenyl)-4H-chromen-4-one. *Indian Journal of Pure and Applied Physics*, 50: 308-313.
21. Costa, J. C., Taveira, R. J., Lima, C. F., Mendes, A. and Santos, L. M. (2016). Optical band gaps of organic semiconductor materials. *Optical Materials*, 58: 51-60.
22. Hegde, H., Sinha, R. K., Kulkarni, S. D. and Shetty, N. S. (2020). Synthesis, photophysical and DFT studies of naphthyl chalcone and nicotinonitrile derivatives. *Journal of Photochemistry and Photobiology A: Chemistry*, 389: 112222.
23. Sánchez-Vergara, M. E., Leyva-Esqueda, E. A., Alvarez, C., López Reyes, M., Miralrio, A. and Salcedo, R. (2016). Influence of TCNQ acceptor on optical and electrical properties of tetrasubstituted allenes films fabricated by vacuum thermal

evaporation. *Journal of Materials Science: Materials in Electronics*, 27(9): 9900-9910.

24. Bureš, F. (2014). Fundamental aspects of property tuning in push–pull molecules. *RSC Advances*, 4(102): 58826-58851.
25. Janardhana, K., Ravindrachary, V., Kumar, P. C., Umesh, G. and Manjunatha, K. B. (2013). Third order optical non-linearity of a novel chalcone derivative through Z scan technique. *Indian Journal of Pure and Applied Physics,* 51: 844-850.
26. Nakum, K. J., Katariya, K. D., Hagar, M. and Jadeja, R. N. (2022). The influence of lateral hydroxyl group and molecular flexibility on the mesogenic behaviour of a new homologous series based on thiophene-chalcone: Synthesis, characterization, crystal structure and DFT study. *Journal of Molecular Structure*, 1261: 132891.
27. Jiang, X., Zhao, S., Lin, Z., Luo, J., Bristowe, P. D., Guan, X. and Chen, C. (2014). The role of dipole moment in determining the nonlinear optical behavior of materials: ab initio studies on quaternary molybdenum tellurite crystals. *Journal of Materials Chemistry C*, 2(3): 530-537.
28. Maidur, S. R., Jahagirdar, J. R., Patil, P. S., Chia, T. S. and Quah, C. K. (2018). Structural characterizations, Hirshfeld surface analyses, and third-order nonlinear optical properties of two novel chalcone derivatives. *Optical Materials*, 75: 580-594.
29. Maidur, S. R., Patil, P. S., Ekbote, A., Chia, T. S. and Quah, C. K. (2017). Molecular structure, second- and third-order nonlinear optical properties and DFT studies of a novel non-centrosymmetric chalcone derivative:(2E)-3-(4-fluorophenyl)-1-(4-{[(1E)-(4-fluorophenyl) methylene] amino} phenyl) prop-2-en-1-one. *Spectrochimica Acta Part A: Molecular and Biomolecular Spectroscopy*, 184: 342-354.
30. Jagadeesh, M., Lavanya, M., Babu, B. H., Hong, K., Ma, R., Kim, J. and Kim, T. K. (2015). Synthesis and detailed spectroscopic characterization of various hydroxy-functionalized fluorescent chalcones: A combined experimental and theoretical study. *Spectrochimica Acta Part A: Molecular and Biomolecular Spectroscopy*, 150: 557-564.
31. Chaudhry, A. R., Irfan, A., Muhammad, S., Al-Sehemi, A. G., Ahmed, R. and Jingping, Z. (2017). Computational study of structural, optoelectronic and nonlinear optical properties of dynamic solid-state chalcone derivatives. *Journal of Molecular Graphics and Modelling*, 75: 355-364.